

## Magnetization process in FePd thin films

O. Klein<sup>a)</sup>

*Service de Physique de l'Etat Condensé, CEA Orme des Merisiers, F-91191 Gif-Sur-Yvette, France*

Y. Samson and A. Marty

*Service de Physique des Matériaux et Microstructures, CEA Grenoble, F-38054 Grenoble, France*

S. Guillous

*Laboratoire des Solides Irradiés, Ecole Polytechnique, Palaiseau F-91128, France*

M. Viret and C. Fermon

*Service de Physique de l'Etat Condensé, CEA Orme des Merisiers, F-91191 Gif-Sur-Yvette, France*

H. Alloul

*Laboratoire de Physique des Solides, Université Paris-Sud, F-91405 Orsay, France*

A custom made magnetic force microscope is used to study the magnetization process in thin films of FePd throughout the entire hysteresis loop. The 40 nm thick sample has a strong perpendicular anisotropy, which leads to a maze of 80 nm wide stripes of opposite polarity in the remanent state. The growth of  $M$ , when  $H$  increases, happens through an unwinding of the reversed domain along their axis. Together with the length recession, the reversed domain width also contracts with increasing field. The later effect is estimated by comparison of our images with magneto-optical Kerr measurements. A large disorder in the propagation process of the domain walls is observed. It is also found that the bubble configuration near the saturation field is unstable. © 2001 American Institute of Physics. [DOI: 10.1063/1.1355326]

Magnetic thin films with perpendicular magnetic anisotropy have been extensively studied since the 1960s because of their potential application as magnetic storage devices. In the case of garnets (the most well-known example) the integration capacity is limited by the micron size of the magnetic domains. Recently there has been a revival of interest in this area with the synthesis of new magnetic layers with very strong perpendicular anisotropy using either ordered alloys<sup>1</sup> or multilayers.<sup>2</sup> Magnetic force microscopy (MFM) studies<sup>1,2</sup> show that the magnetic domains in these materials are in the tens of nanometers scale range in the remanent configuration ( $B=0$ ). But it is often the magnetization reversal process or domain wall mobility<sup>3</sup> that determines the suitability for applications, like in magneto-optical devices where only the domain wall coercitivity prevents the collapse of the recorded information. Here, we report on the observation of the domain configuration along the hysteresis cycle in thin FePd layers. We use a homemade MFM instrument to image the sample up to the saturation field (around 0.5 T).

The microscope is located between the poles of a  $\pm 1$  T electromagnet which applies a homogeneous static field  $H$  perpendicular to the sample surface at room temperature. The mechanical probe is a  $\text{Si}_3\text{N}_4$  commercial cantilever of spring constant  $k=0.01$  N/m coated with 30 nm of  $\text{Co}_{0.8}\text{Cr}_{0.2}$ . The film is sputtered exclusively at the extremity of the sensor to avoid spurious bending during the deposition process. The deposit is subsequently magnetized in the direction of the applied field. The signal is measured by a beam deflection system that reflects off the rear side of the cantilever onto a position sensor. The images are acquired in

static scanning mode where the measured signal is the magnetic force acting on the tip. The cantilever is scanned without feedback control in a plane parallel to the surface with a tip-sample separation of approximately 50 nm. The acquisition time of each image is several minutes long. The applied field is measured by a Hall sensor calibrated against a nuclear magnetic resonant signal.

The sample is a 40 nm thick FePd alloy layer grown epitaxially where Fe and Pd are coevaporated from two independent sources on a MgO(001) substrate held at 620 K. This process leads to a high uniaxial chemical ordering within the  $L1_0$  phase and then to a strong perpendicular anisotropy (quality factor:  $Q=2K_u/(2\pi M_s^2)=1.8$ ,<sup>1</sup> with  $M_s$  the saturation magnetization and  $K_u$  the magnetocrystalline anisotropy). The zero field domain pattern consists of a maze of alternating up and down domains which is understood as the result of a competition between the magnetostatic energy which favors small domains and the energy cost associated with the creation of domain walls  $\sigma_w$ . The equilibrium width depends on the film thickness with a minimum for  $t \sim 40$  nm,<sup>1</sup> the size used in this work.

We first study how the domain configuration evolves throughout the magnetization process. Figure 1 shows MFM images of the same location at different field values when increasing the applied field while Fig. 2 shows the magnetization reversal in decreasing field. For all our images, the contrast corresponds to a reversal of the perpendicular stray field indicating a change in the domain polarity.<sup>4</sup> The black and white stripes are, respectively, the domains aligned and reversed with the field. An enhancement of the force contrast is observed in increasing field.<sup>4</sup> The stray field from the tip does not seem to affect the domain configuration. Indeed, the images are identical whatever the scan direction (the image

<sup>a)</sup> Author to whom correspondence should be addressed; electronic mail: oklein@cea.fr

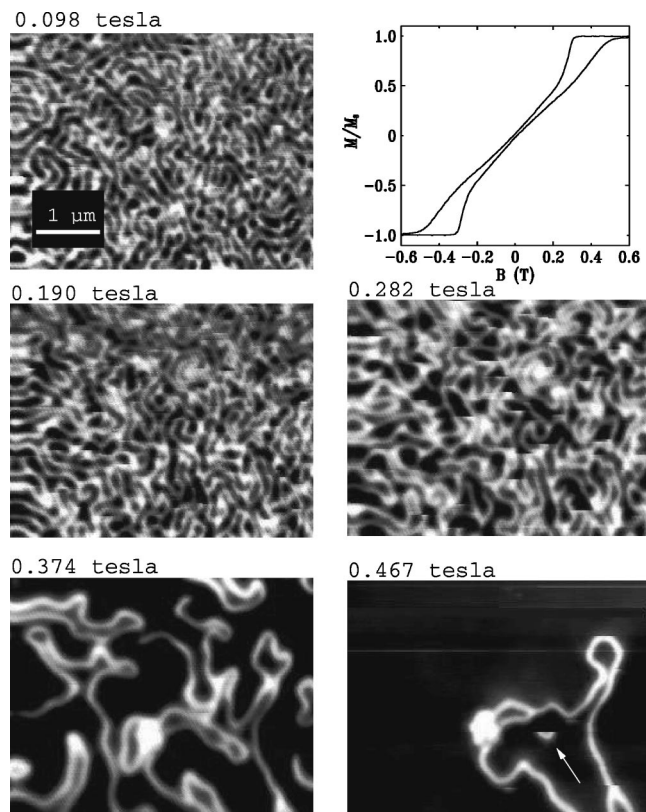


FIG. 1. Magnetization process imaged by MFM in increasing magnetic field. The white stripes are the reversed domains. The scan area is a  $5 \times 4 \mu\text{m}^2$  surface with the fast scan direction aligned along the horizontal axis. A domain movement induced by the tip can be seen in the bottom image (arrow). The upper part shows the normalized hysteresis loop of our sample obtained by MOKE with the field applied perpendicular to the layer.

at 0.467 T in Fig. 1 illustrates a scarce event of wall motion induced by the tip). At  $B=0$ , the local period gives access to the domain width, equal to 80 nm. Upon approaching saturation, the size of the dark regions increases rapidly. A resemblance, however, between the patterns of each image is perceived, as most of the walls remains undisplaced in spite of local modifications of the demagnetizing field. In garnets, the standard reorganization process includes a straightening of the domain walls.<sup>5</sup> Here, the growth of  $M$  is mainly allowed by a diminution of the length of the reversed domain causing them to roll back from their extremities. This is seen as an indication of a large coercivity preventing their motion.

The bubble state near the saturation field could not be imaged by our instrument. Considering the scanned sizes, this is a likely indication that the bubble configuration is unstable on the imaging time scale (MFM tip field can additionally destabilize bubbles). Also nucleation events seem a rather rare process, while domain wall propagation ensures most of the magnetization reversal with a dynamics that is much faster than the acquisition time. For instance in Fig. 2, the white stripes, which are connected, emerge from the same nucleation center located out of the observed area. The domain repartition is even more inhomogeneous than in Fig. 1. This is controlled by local magnetic inhomogeneities opposing wall motion.<sup>6</sup> In contrast to observation performed in

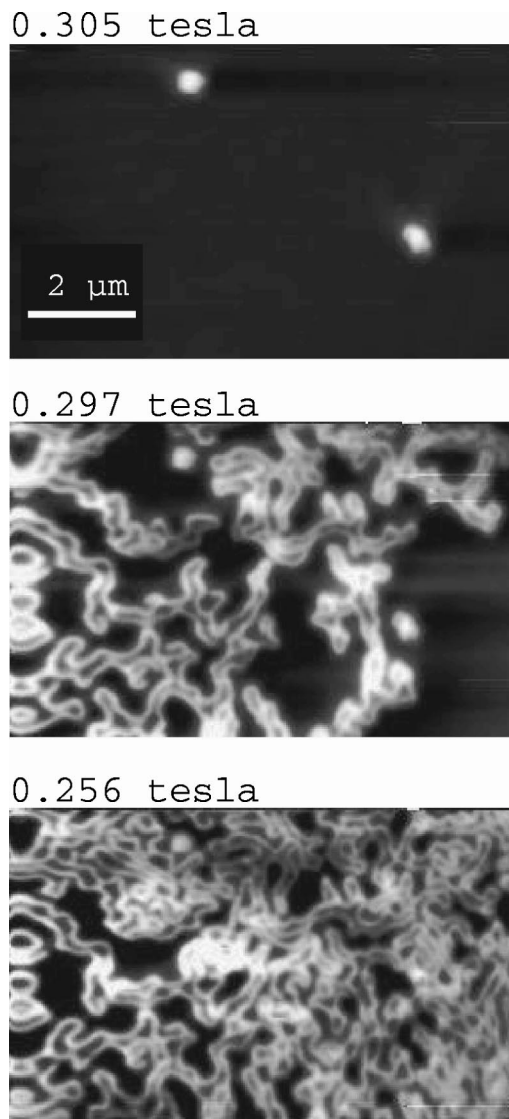


FIG. 2. Nucleation process imaged by MFM in decreasing magnetic field. The scan area is a  $10 \times 6 \mu\text{m}^2$  surface.

garnets, the domain propagation does not adopt a starlike shape but rather proceeds from a single stripe with only rare branching events.

At high fields, pointlike reversed regions are still observed above 0.5 T. Two of these anomalies are visible on the 0.305 T picture in Fig. 2. The location of these spots is independent of the magnetic field history. Furthermore, these spots still appear as minority domain when the applied field is inverted. As a result, they are attributed to magnetic anomalies localized on structural defects. Surprisingly, these defects rarely participate in the nucleation process as demonstrated in Fig. 2. Their measured diameter is 130 nm and this value is independent of the defects observed, but it changes if the tip is replaced. We believe that the image of quasipunctual magnetic defects is the force transfer function of our magnetic tip and the 130 nm diameter reflects the width of our probe in MFM mode. This figure is much greater than the physical size of the apex of the tip (around 30 nm, as obtained from the apparent width of a selected 10 nm carbon nanotube measured in both AFM contact mode

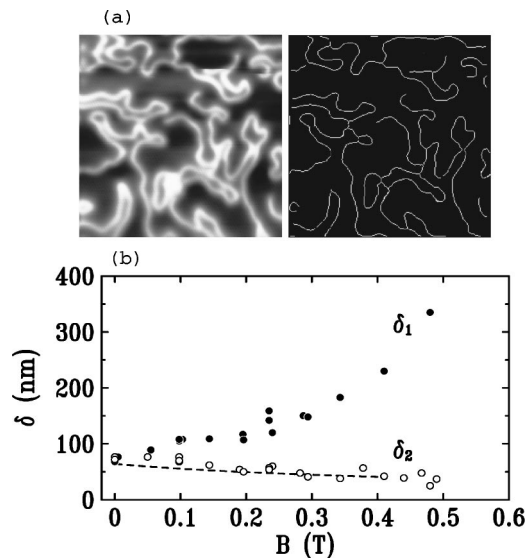


FIG. 3. (a) Illustration of the image treatment used to infer the width of the reversed domains  $\delta_2$ . The MFM image is transformed through a function which returns the set of skeletal pixels at the medial axis of the white stripes. From the length of the reversed region,  $\delta_2$  is calculated by setting the magnetization of the image equals to the MOKE value. The result is shown in (b). The dashed line is the behavior predicted by the Kooy and Enz model (Ref. 5) with no adjustable parameters.

and by TEM). This discrepancy is not surprising, since magnetic stray fields have a relatively smooth spatial decay. Therefore some of the magnetic charge deposited on the faces of the pyramid above the tip apex contributes to the signal and produces a deterioration of the spatial resolution.<sup>4</sup> Nevertheless, the low field image clearly demonstrates that the same tip can resolve 80 nm wide domains.<sup>7</sup> It also explains why the force contrast diminishes at low fields. Finally, we observe that these spots are all present up to 1.1 T, although a progressive decrease of the force contrast is measured in strong fields, presumably because the diameter of these magnetic anomalies diminishes with increasing field.

From the previous discussion, we conclude that the width  $\delta_2$  of the reversed region cannot be inferred directly from the image, except in the case of alternating stripes of equal width ( $B=0$ ). The force signal is a convolution of the sample stray field with the sensor size. This leads to an overestimation of the width of the minority domains. This effect could cause an apparent discrepancy between MFM measurements and bulk characterizations.<sup>3</sup>

We make the approximation that images are large enough so that the magnetization value measured at this scale be close to the bulk value (see Fig. 1) obtained by magneto-optic Kerr effect (MOKE). This approximation may break down near saturation, when the domain pattern is highly inhomogeneous. From the images, it is possible to extract properly the length of the reversed domains  $\ell_2$  inside the scanned area (see Fig. 3). Next we can obtain their width  $\delta_2 = (1 - M/M_s)A / (2\ell_2)$  from the magnetization in Fig. 1 with  $A$  the scanned area. The field dependence of  $\delta_2$  is plotted in Fig. 3. It is found that  $\delta_2$  decreases from 80 nm at  $B=0$  to  $\sim 40$  nm at  $B=0.5$  T. This dependence is compared

with the behavior predicted by the model of Kooy and Enz.<sup>5</sup> Here, we use the magnetic parameters of FePd ( $K_u = 1.2 \times 10^7$  erg/cm<sup>3</sup>,  $M_s = 1030$  emu/cm<sup>3</sup>,  $D_0 = 16$  nm, the dipolar length,<sup>1</sup> and  $t = 40$  nm, the film thickness) with no adjustable variables. The prediction results is the dashed line in Fig. 3. From the  $\delta_2$  value, one can define  $\delta_1 = \delta_2(1 + M/M_s)/(1 - M/M_s)$ , a parameter that can be identified as the width of the favored domains. The field dependence of  $\delta_1$  (increasing field only) is also shown in Fig. 3. The divergence indicates the position of the saturation field  $B_s$ . Here  $B_s$  that is inferred from MFM images is in good agreement with the MOKE measurements. Noticeably the model<sup>5</sup> underestimates  $B_s$ . This can be explained as it relies on equilibrium calculations and leaves apart the various sources of the hysteresis.<sup>8</sup>

We have measured the variation of the force signal with the tip to sample separation. As predicted for two-dimensional arrays uniformly magnetized in the thickness, we find that the force signal decays exponentially, and the damping coefficient is equal to the domain spatial frequency  $1/(\delta_1 + \delta_2)$  calculated above.<sup>9</sup> This agreement breaks down for large periods as the decay coefficient becomes field independent. In our case, the crossover value occurs at  $(\delta_1 + \delta_2)/2 = 125$  nm. Such a result is consistent with our tip dimension estimated previously. A final point should be made: Since the decay of the stray field depends on the domain periodicity, one expects that the width of the force transfer function of our magnetic tip increases for increasing magnetic period. This is why, on the images, the magnetic anomalies appear both larger and stronger than the domains despite the fact that their size is smaller.

In conclusion, the magnetization process of FePd thin films has been observed by MFM. The growth of  $M$ , when  $H$  increases, occurs through a rollback of the ends of the reversed domains along their axis. This process is associated with a width contraction which is quantitatively estimated and the field dependence compares favorably with the model of Kooy and Enz. A large disorder in the propagation process of the domain walls is observed, leading to highly inhomogeneous magnetic patterns. It is also found that the bubble configuration near the saturation field is unstable.

The authors are greatly indebted to J. Ferré for his help in some of the Kerr experiments. They would also like to thank F. Ott for stimulating discussions. This research was partially supported by the Ultimatech Program of the CNRS.

<sup>1</sup>V. Gehanno *et al.*, J. Magn. Magn. Mater. **172**, 26 (1997).

<sup>2</sup>L. Belliard *et al.*, J. Appl. Phys. **81**, 5315 (1997).

<sup>3</sup>J. Schmidt, G. Skidmore, S. Foss, E. Dahlberg, and C. Merton, J. Magn. Magn. Mater. **190**, 81 (1998).

<sup>4</sup>P. J. A. van Schendel, H. J. Hug, B. Stiefel, S. Martin, and H.-J. Güntherodt, J. Appl. Phys. **88**, 435 (2000).

<sup>5</sup>C. Kooy and U. Enz, Philips Res. Rep. **15**, 7 (1960).

<sup>6</sup>T. Pokhil, B. Vvedensky, and E. Nikolaev, Mater. Sci. Forum **62-64**, 619 (1990).

<sup>7</sup>The ability of an instrument to resolve regular patterns of small periods is mainly an indication of its force sensitivity and not of its spatial resolution performance.

<sup>8</sup>I. S. Weir, J. N. Chapman, I. S. Molchanov, D. M. Titterton, and J. Rose, J. Phys. D **32**, 395 (1998).

<sup>9</sup>J. Mallinson, IEEE Trans. Magn. **17**, 2453 (1981).